Thermodynamic and topological phase diagrams of correlated topological insulators

Damian Zdulski and Krzysztof Byczuk
Faculty of Physics, Institute of Theoretical Physics, University of Warsaw, ul.Pasteura 5, PL-02-093 Warsaw, Poland
(Received 30 April 2015; published 1 September 2015)

A definition of topological phases of density matrices is presented. The topological invariants in case of both noninteracting and interacting systems are extended to nonzero temperatures. The influence of electron interactions on topological insulators at finite temperatures is investigated. A correlated topological insulator is described by the Kane-Mele model, which is extended by the interaction term of the Falicov-Kimball type. Within the Hartree-Fock and the Hubbard I approximations, thermodynamic and topological phase diagrams are determined where the long-range order is included. The results show that correlation effects lead to a strong suppression of the existence of the nontrivial topological phase. In the homogeneous phase, we find a purely correlation driven phase transition into the topologically trivial Mott insulator.

DOI: 10.1103/PhysRevB.92.125102 PACS number(s): 03.65.Vf, 71.10.Fd, 71.10.Hf, 71.27.+a

I. INTRODUCTION

Recently discovered topological insulators (TIs) have attracted a lot of interest in condensed matter physics [1–6]. This novel electronic phase in solids has a band gap in the bulk but it can conduct an electric current via gapless edge states, which are robust against scattering on impurities or other weak perturbations of ideal systems [7]. The formation of the metallic edge states is related to the nontrivial topology of the ground state, which originates from a spin-orbit coupling [8]. The TIs are characterized by topological invariants which cannot be continuously changed unless the single-particle gap is closed [7]. The idea of the TIs has been extended into symmetry protected topological phases, which possess nontrivial topological properties as long as the symmetries are present [8]. The existence of the topological gapless edge states was experimentally confirmed by transport measurements [9–12] and an angle-resolved photoemission spectroscopy [10,13–15] in many materials, such as, e.g., Bi_2Se_3, $Pb_{1-x}Sn_xSe$, or HgTe/CdTe quantum wells.

The existence of the TIs and most of their properties can be understood and described within the noninteracting band theory. Recently, an influence of electron-electron interactions on the topological insulating states has attracted a growing attention [16]. Theoretical studies are focused mainly on two effects of the strong correlations in topologically nontrivial conditions. The first effect is when a non-on-site interaction yields new topological phases [17]. The second problem is how strong correlations change the properties of the band topological insulators. Namely, interaction can lead to the creation of an ordered phase, which through renormalization of the band parameters may compete with the topological state [16,18]. Moreover, local correlations related to the frequency dependent part of the self-energy can drive a topological phase transition [19–21]. These issues have been stimulated by research on iridium-based materials X_2IrO_3 (X = Na or Li) in which both spin-orbit coupling and electron correlations are strong [22]. Another new class of systems in which strong interactions could play an important role are cold atoms in optical lattices [23]. Recent experimental progress in this field allows to test Hamiltonians with different types of hoppings on lattices, synthetic spin-orbit couplings, and synthetic gauge fields, as well as the interactions, in terms of their topological properties [24,25].

Despite of intensive research, the influence of the strong correlations on the TIs at finite temperatures appeared so far only in few studies [26–29]. A major problem was how to extend the idea of the topological insulators to nonzero temperatures. Main progress in this field was made in Ref. [30] were the concept of topological phases of density matrices was introduced. However, it is still not known how the correlations affect the behavior of the TIs at nonzero temperatures and how to compute topological invariants of interacting systems in these cases.

In this work, we investigate the phase diagram of the correlated TIs at finite temperatures. Using the concept of topological phases for density matrices, we introduce methods to compute topological invariants for noninteracting and interacting systems at nonzero temperatures. Then, we consider the Kane-Mele (KM) model without the Rashba spin-orbit coupling term [1]. To include correlations, we extended the KM model by adding an interaction term as in the Falicov-Kimball (FK) model. It describes a short-range local Coulomb interaction between itinerant electrons and localized spinless fermions [31]. We employ the Hartree mean-field and Hubbard I approximations to study the phase transitions and obtain the phase diagrams. This approach allows us to obtain semianalytical results for topological phase transitions and examine the influence of the electronic correlations at finite temperatures. Optical lattices offer the possibility of a physical realization of this model [23]. A similar model has been investigated in Ref. [32] within the dynamical mean-field approximation (DMFT) [33,34]. However, the long-range ordered phases have not been discussed in general cases [32].

The paper is structured as follows. In Sec. II, we present the extension of topological invariants to finite temperatures. In Sec. III, we introduce the KM model with the FK type interaction. We present the condition for a change of a topological invariant in the system in Sec. IV, and in Sec. IV B we describe the Hartree and Hubbard I approximations. In Sec. V, we examine thermodynamic phase diagrams with topological phases. In Sec. VI, we present our conclusions.

II. TOPOLOGICAL PHASES AT NONZERO TEMPERATURES

A. Topological phases of the density matrices

At a nonzero temperature, the system is no longer in a ground state and there is a general problem how to define and interpret topological invariants. When the electron correlations are absent, the topological phases of insulators at zero temperature can be defined as homotopy equivalence classes of mappings $\mathbf{k} \mapsto H(\mathbf{k})$, from a Brillouin zone (BZ) torus T^d to a manifold of the gapped Bloch Hamiltonians (BHs) [8,35]. For symmetry protected TIs, points of the manifold represent preservation of the symmetry gapped BHs.

At a nonzero temperature, a quantum system is described by a density matrix ρ of a mixed state. For translational invariant systems without electron correlations, the density matrix takes the form $\rho = \prod_{\mathbf{k}\in BZ} \rho(\mathbf{k})$, where $\rho(\mathbf{k})$ is called the Bloch density matrix (BDM). In order to extend the notion of topological invariants to nonzero temperatures and nonequilibrium systems, topological phases for the BDMs have been defined by using an ensemble of nonorthonormalized pure states, cf. Ref. [30].

We express this definition in an equivalent but more convenient for our purposes form, which is analogous to the BHs, i.e., the homotopy equivalence relation of the BDMs with a constrain that the spectral gap between the valence band eigenvalues $p_v(\mathbf{k})$ of $\rho(\mathbf{k})$ and the conduction band eigenvalues $p_c(\mathbf{k})$ cannot be closed, and protecting symmetries must be preserved during a homotopy transformation. Formally, we can use the following definitions.

Definition 1. Let $\rho(\mathbf{k})$ and $q(\mathbf{k})$ be Bloch density matrices of size N of a d-dimensional system. Additionally, let the corresponding to them density matrices be invariant under a symmetry group G. They are said to be topologically equivalent, written as $\rho(\mathbf{k}) \sim q(\mathbf{k})$, if there exist a continuous map $F : T^d \times [0,1] \mapsto D_N(N)$, such that:

$$(i)\ \ \forall_{\mathbf{k}}\,\{F(\mathbf{k},0) = \rho(\mathbf{k}) \wedge F(\mathbf{k},1) = q(\mathbf{k})\},$$

$$(ii)\ \ \forall_{t\in[0,1]}\,\forall_{\mathbf{k}}\,\{p_v(\mathbf{k},t) - p_c(\mathbf{k},t) > 0\},$$

$$(iii)\ \ \forall_{g\in G}\forall_{t\in[0,1]}\,[F(t),U(g)] = 0,$$

where $F(t)$ is the density matrix corresponding to the BDM $F(\mathbf{k},t)$. The eigenvalue $p_{v(c)}(\mathbf{k},t)$ is defined as the $n\,(n+1)$th largest eigenvalue of the $F(\mathbf{k},t)$, where the number n is determined by a physical parameter describing occupation of states. In the case of equilibrium systems, it is the chemical potential μ. It is a generalization of the definition for the BHs, where the valence and conduction bands $E_{v(c)}(\mathbf{k})$ can be defined as the $n\,(n+1)$th lowest eigenvalue of $H(\mathbf{k})$. The operator $U(g)$ describes a symmetry operation $g \in G$. The space of the BDMs is labeled as $D_N(N) \equiv GL(\mathbb{C},N)/U(N)$. It is the manifold of strictly positive matrices of size $N \times N$, because topological properties are insensitive to scaling [30] and thereby the normalization condition of BDMs can be omitted.

Definition 1 applies to general BDMs and therefore describes the topological phases for both thermal and nonequilibrium states [36,37]. The spectral constrain (ii) in definition 1 plays a crucial role. From this constrain, it follows that to change the topological phase it is necessary to close a spectral gap or break a protecting symmetry. As a consequence of that, if two topologically nonequivalent systems belonging to the same symmetry class are connected, on the interface between them, the transformation $F(\mathbf{k},t)$ evolves through a region of the space $D_N(N)$ where the spectral gap disappears and thereby edge states occur. These states are insensitive to small perturbations preserving the protecting symmetry. Therefore the spectral constrain (ii) establishes the bulk-boundary correspondence as in the case of BHs.

Without the spectral constrain (ii), we can always deform by means of a transformation $F(\mathbf{k},t)$ all BDMs to the maximally mixed one and in that case there exists only the topologically trivial phase. The spectral constrain is not present when all possible states are fully occupied. This entails that the sum of topological invariants of all bands must be zero.

B. Topological invariants at finite temperatures

We show that definition 1 provides for every finite temperature the same classification of the topological phases and formulas for the topological invariants as for BHs.

1. Noninteracting systems

In equilibrium state, the BDM takes the form

$$\rho(\mathbf{k}) = \frac{e^{-\beta H(\mathbf{k})}}{Z}, \tag{1}$$

where $Z^M = \mathrm{Tr}(e^{-\beta H})$, H is the full Hamiltonian, β is the inverse of the temperature T, and M is the number of unit cells. Hence, for every T, Eq. (1) establishes a one-to-one correspondence

$$\varphi : H(\mathbf{k}) \mapsto \rho(\mathbf{k}) \tag{2}$$

preserving the protecting symmetries and the spectral gap, i.e., $p_c(\mathbf{k}) = p_v(\mathbf{k})$ if and only if $E_c(\mathbf{k}) = E_v(\mathbf{k})$. As a consequence of that, if two insulators belong to the same topological class of BHs, they must be in the same topological phase of BDMs and thereby φ is the isomorphism of equivalence classes of topological insulators. Therefore possible topological phases of finite temperature BDMs have the same classification as in the periodic table of topological insulators and superconductors [6] and the topological invariants are computed by substituting

$$\varphi^{-1}(\rho(\mathbf{k})) = -\frac{1}{\beta}\ln(Z\rho(\mathbf{k})) \tag{3}$$

into the place of $H(\mathbf{k})$ in the standard formulas for the topological invariants [6,7]. In the limit $T \to \infty$, this theorem is not valid because φ is not injective function, i.e., it does not preserve the distinctness of elements. In that case, the system is always described by a maximally mixed density matrix, and thereby it is in the topologically trivial state.

2. Interacting systems

There is not known a general classification of topological insulators for all interacting systems. Therefore the existing in literature topological invariants for interacting systems are constructed as an analytical continuation of the formulas for

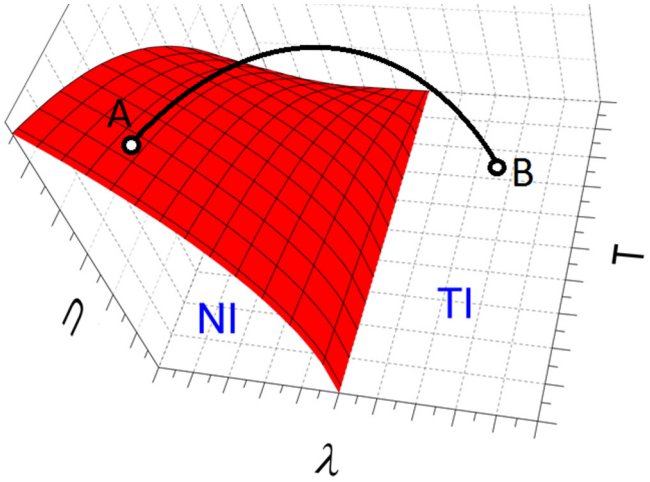

FIG. 1. (Color online) Exemplary topological phase diagram in the space of interaction U, temperature T, and parameter λ. The red surface is the phase boundary separating the normal insulator (NI) and topological insulator (TI). The curve AB connects adiabatically two points.

noninteracting systems [8,38]. For interacting systems, the Hamiltonian cannot be expressed as a single-particle operator. Therefore, in order to perform an analytical continuation of the noninteracting topological invariants, they must be formulated in terms of a single-particle Green's function G [38], i.e.,

$$G^{-1}(\omega,\mathbf{k}) = \omega I - H(\mathbf{k}), \tag{4}$$

where ω is the frequency and I is the unity operator. This generalization of topological invariants describes properly topological phases until the interacting system is continuously connected in the space of parameters of the model to some noninteracting system without closing the spectral gap. Hence this description cannot be applied to fractional topological insulators.

With the additional assumption that T is treated on the same footing as the parameters of the model, the above construction can be generalized to the density matrices. This entails that the interacting system can be adiabatically connected to a noninteracting one with a different temperature, which is illustrated by the line AB in Fig. 1.

As it was discussed in the Sec. II B 1, all formulas for the noninteracting topological invariants are identical for BHs and BDMs due to the isomorphism from Eq. (2). Therefore, by substituting Eq. (3) in place of $H(\mathbf{k})$ in Eq. (4), the topological invariants expressed by $G(\omega,\mathbf{k})$ can be calculated for the BDMs. The analytical continuation to interacting systems does not break this correspondence and thereby the same statements hold for the topological invariants of the interacting systems. In particular, also the concept of topological Hamiltonian [39,40] remains unchanged for the density matrices.

C. Interpretation of topological invariants at finite temperatures

In recently published papers, see Refs. [41,42], a different extension of the concept of topological invariants to finite temperatures is proposed. Those topological invariants do not match with these derived here from definition 1. In contrast to our proposal, those topological invariants depend explicitly on a temperature for noninteracting systems. Additionally, it is shown in Ref. [30] that they are not unique. Another advantage of definition 1 is that due to the bulk-boundary correspondence the spectral constrain (ii) links our topological invariants to the physical observable, which is the number of edge states.

Finally, we note that at nonzero temperatures, the quantum Hall conductivity is not quantized due to a thermal activation of states from a conduction band. Therefore the topological invariants cannot be measured directly as response functions. However, at sufficiently low temperatures, the contribution from the topological edge states should dominate. An effect that can identify a nontrivial topological phase at finite temperatures is the spin-charge separation in the presence of certain topological defects [43,44]. When a topological insulator is threaded by magnetic π fluxes, midgap spinon and chargon localized states occur. They have Curie law susceptibilities at sufficiently low temperatures when the bulk contributions do not dominate [45]. An advantage of this approach is that it is not based on the adiabatic connection to a noninteracting system and hence it can also be used to identify interaction induced topological phases at finite temperatures. On the other hand, the edge states are experimentally accessible by angle-resolved photoemission spectroscopy even at room temperature [10,46].

III. MODEL

As discussed in Sec. II, the topological invariants for noninteracting systems at finite and zero temperature are the same when the parameters of the model are not temperature dependent. The situation is more complex in case of correlated systems because the temperature change of the order parameter affects the self-energy of the electrons and hence the topological properties of the system. To investigate this effect, we use the KM model [1]. It is represented by a Hamiltonian whose eigenstates exhibit the quantum spin Hall effect [47]. Formally, it is constructed from two copies of the Haldane model [48] with opposite signs of the Peierls phase for the electrons with the up and down spins, respectively, moving on a honeycomb lattice. We extend this model by adding localized spinless fermions, which locally interact with the itinerant electrons as in the FK model [31]. The full Hamiltonian is

$$H = -t_1 \sum_{\langle i,j\rangle\sigma} c^\dagger_{i\sigma} c_{j\sigma} - t_2 \sum_{\ll i,j\gg\sigma\sigma'} e^{i\phi_{ij}} c^\dagger_{i\sigma} \tau^z_{\sigma\sigma'} c_{j\sigma'} + U \sum_{i\sigma} \left(c^\dagger_{i\sigma} c_{i\sigma} - \frac{1}{2}\right)\left(f^\dagger_i f_i - \frac{1}{2}\right), \tag{5}$$

where $c_{i\sigma}$ ($c^\dagger_{i\sigma}$) is the annihilation (creation) operator for the itinerant electron with the spin $\sigma =\uparrow$ ($\downarrow$), and f_i ($f^\dagger_i$) is the annihilation (creation) operator for the localized spinless fermion at the lattice site i. The parameter $t_1 > 0$ is the nearest-neighbor hopping, whereas $t_2 > 0$ is the amplitude of the next-nearest-neighbor hopping. We use $t_1 = 1$, which sets the energy units. The Peierls phase is $\phi_{ij} = \pm\frac{\pi}{2}$ for the next-nearest-neighbor hopping in the clockwise and anticlockwise direction, respectively. The third Pauli matrix is $\tau^z_{\sigma\sigma'}$ and it describes the change of the sign in the Peierls phase for

the electrons with opposite spins. The strength of the local FK interaction is given by U. In this work, we consider a half-filling, i.e., one particle per unit cell for both kinds of fermions. Then the chemical potentials for the itinerant (μ_c) and localized (μ_f) particles are $\mu_c = \mu_f = 0$. The Hamiltonian is invariant with respect to the lattice inversion, the spin rotation, the time reversal symmetry, and the particle-hole transformation. Due to particle-hole symmetry, the system does not possess an indirect band gap for any parameters.

The localized particles in the FK model are thermodynamically coupled to the itinerant electrons and their spatial distributions is determined by a minimum of the thermodynamic potential of the system. On a bipartite lattice at half-filling, the solution of the Kane-Mele Falicov-Kimball (KMFK) model, Eq. (5), with $t_2 = 0$ possesses a long-range order at low temperatures [49], in which the localized fermions form a checkerboard pattern and the itinerant electrons form a charge density wave (CDW). Then the inversion symmetry of the ground state is broken. The transition between the CDW phase and the homogeneous phase is continuous. The order parameter is $d \equiv (n_B - n_A)$, where n_α is the average number of localized particles per unit cell in the sublattice $\alpha = $ A or B. Increasing the hopping amplitude t_2 can lead to a change of the ground state [50]. We estimate that the CDW phase is stable for $t_2 \leqslant 0.5t$ for an arbitrary U (see Appendix A). Therefore we only present results for this regime of the t_2 hopping parameter.

IV. TOPOLOGICAL PHASE TRANSITION

A. General conditions

Topological phases are quantified by topological invariants. For model (5), its topological properties are fully determined by a topological invariant equivalent to the Chern number C for a single spin subsystem [51]. In the noninteracting limit and $t_2 > 0$, the system is in a topologically nontrivial phase with two edge states for open boundary conditions [1].

In order to study the topology of the solution for model (5) with finite U, we introduce the one-particle Green's function $G_\sigma(\omega,\mathbf{k};d)$, which depends implicitly on the order parameter d for the CDW phase. The Green's function obeys the Dyson equation

$$G_\sigma^{-1}(\omega,\mathbf{k};d) = (\omega + \mu_c)I - H_{0\sigma}(\mathbf{k}) - \Sigma_\sigma(\omega,\mathbf{k};d), \quad (6)$$

where

$$\Sigma_\sigma(\omega,\mathbf{k};d) = \begin{pmatrix} \Sigma_{\sigma A}(\omega,\mathbf{k};d) & 0 \\ 0 & \Sigma_{\sigma B}(\omega,\mathbf{k};d) \end{pmatrix}$$

is the diagonal self-energy matrix of the interacting system and $H_{0\sigma}(\mathbf{k})$ is a matrix representation of the noninteracting Hamiltonian. From the theorem discussed in Sec. II B it follows that the topological invariant at every finite temperature for our interacting system is determined by using the standard method [6] applied to the topological Hamiltonian defined by the noninteracting Hamiltonian matrix and the self-energy at $\omega = 0$ [39,40], i.e.,

$$H_\sigma^{\text{top}}(\mathbf{k};d) = H_{0\sigma}(\mathbf{k}) + \Sigma_\sigma(\omega = 0,\mathbf{k};d). \quad (7)$$

We introduce symmetric and antisymmetric combinations of the self-energies

$$\Sigma_{\sigma\text{S/R}}(\mathbf{k};d) = \frac{\Sigma_{\sigma A}(0,\mathbf{k};d) \pm \Sigma_{\sigma B}(0,\mathbf{k};d)}{2},$$

then the topological Hamiltonian for the spin σ particles reads

$$H_\sigma^{\text{top}}(\mathbf{k};d) = H_{0\sigma}(\mathbf{k}) + \Sigma_{\sigma\text{S}}(0,\mathbf{k};d)I + \Sigma_{\sigma\text{R}}(0,\mathbf{k};d)\tau^z. \quad (8)$$

The last term breaks explicitly the inversion symmetry. In the rest of the paper, we use local approximations in which the self-energy does not depend on the wave vector $\mathbf{k}$, i.e., $\Sigma_{\sigma\text{S/R}}(\mathbf{k};d) = \Sigma_{\sigma\text{S/R}}(d)$ is only a function of the order parameter d.

The occurrence of the topologically nontrivial phase is connected with the fact that we cannot choose one global gauge for the eigenvectors of the Hamiltonian matrix (8) that is continuous and single valued over the whole BZ [52]. This yields the condition

$$|\Sigma_R(d)| > 3\sqrt{3}t_2 \quad (9)$$

for the transition from the topological phase to the trivial phase (see Appendix B). We note that this is a general condition for the existence of nontrivial topology for any local approximation.

B. Considered approximations

1. *Hartree approximation*

Within the Hartree approximation, the self-energy (6) of the itinerant particles is given by [53]

$$\Sigma_\sigma(\omega,\mathbf{k};d) = \begin{pmatrix} U\,n_A & 0 \\ 0 & U\,n_B \end{pmatrix}. \quad (10)$$

Hence

$$\Sigma_{\sigma R}(d) = -\frac{Ud}{2}, \quad (11)$$

and from Eq. (9), the condition for the change of the topological invariant takes the form

$$U > U_c^{\text{H}} = \frac{6\sqrt{3}t_2}{|d|}. \quad (12)$$

The Hartree approximation corresponds to the first-order perturbation expansion with respect to small U.

2. *Hubbard I approximation*

Within the Hubbard I approximation, the self-energy (6) of the itinerant particles is given by [53]

$$\Sigma_\sigma(\omega,\mathbf{k};d) = \begin{pmatrix} U\,n_A + \frac{U^2 n_A n_B}{\omega + U(\frac{1}{2} - n_B)} & 0 \\ 0 & U\,n_B + \frac{U^2 n_B n_A}{\omega + U(\frac{1}{2} - n_A)} \end{pmatrix}. \quad (13)$$

Hence

$$\Sigma_{\sigma\text{R}}(d) = -\frac{Ud}{2} - \frac{U(1-d^2)}{2d} = -\frac{U}{2d}. \quad (14)$$

There are two contributions to Eq. (14): (i) the Hartree term, which takes into account a formation of the long-range order; and (ii) the term that takes into account effects of local electron

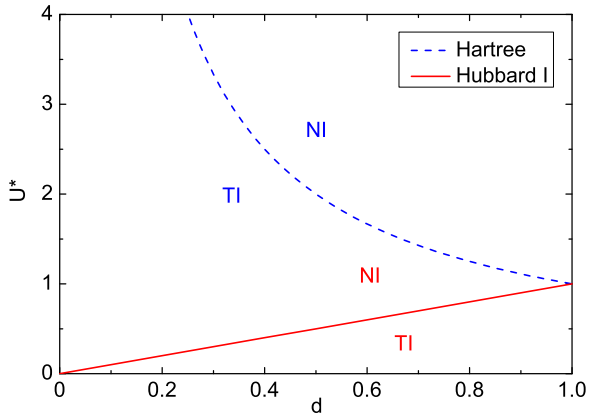

FIG. 2. (Color online) Topological phase diagram of KMFK model within the Hartree (blue line) and Hubbard I (red line) approximations in the space of (d, U^*) parameters, where $U^* = U/6\sqrt{3}t_2$, TI stands for topological insulator, and NI for normal insulator.

correlations. Substituting $\Sigma_{\sigma \mathrm{R}}$ into Eq. (9), the condition for the change of the topological invariant takes the form

$$U > U_c^{\mathrm{HI}} = 6\sqrt{3}t_2|d|. \tag{15}$$

The Hubbard I approximation becomes exact when we neglect t_1 hopping and t_2 amplitudes.

C. Topological phase diagrams

In both Eqs. (12) and (15), the critical interaction strength U_c depends linearly on t_2. For $|d| = 1$, the correlation term in (14) vanishes and $U_c^{\mathrm{HI}} = U_c^{\mathrm{H}}$. For $|d| < 1$, the critical interaction U_c^{H} increases with decreasing $|d|$, whereas U_c^{HI} vanishes linearly with decreasing $|d|$, cf. Fig. 2. Since the electronic correlations are included within the Hubbard I approximation, we conclude that they reduce strongly the topologically nontrivial solution. This is due to the formation of additional band states inside the Hartree gap, as is shown in Fig. 3, because of the frequency dependence of the self-energy (13). This results in a closed energy gap for smaller U in comparison to the Hartree approximation case and thereby the topological invariant is changed.

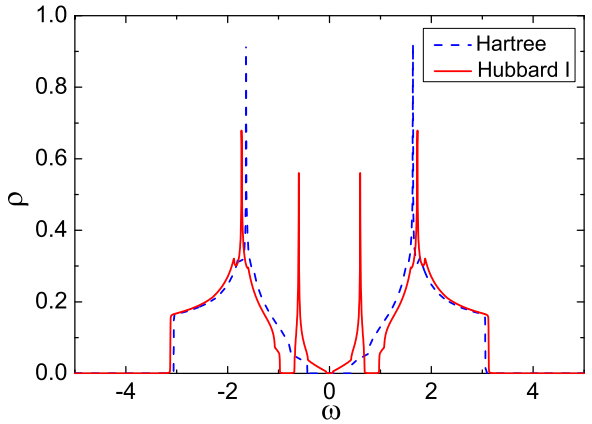

FIG. 3. (Color online) Density of states of KMFK model within the Hartree and Hubbard I approximations. We use $t_2 = 0.2, U = 1.5$, and $d = 0.8$.

In a homogeneous phase with $d = 0$, the noninteracting model has a topological insulating phase. For any finite interaction $U > 0$, the Hubbard I solution gives a topologically trivial Mott insulator. It means that $U = 0$ is a singular point in this approximation. The transition from the topological insulator to the normal Mott insulator occurs without closing the band gap and it is only driven by local correlations. We find that in the Hubbard I approximation $\Sigma_R(d \to 0) = \infty$ for any $U > 0$. However, the analytical condition (15) remains well defined if we take the $d \to 0$ limit at the end. Then, we do not have to use the concept of the frequency domain winding number [54] to compute the topological invariant in the homogeneous phase.

D. More advanced approximations

In Fig. 2, we see that the Hartree and Hubbard I solutions diverge from each other when the homogeneous phase is approached. Mathematically, it is due to the fact that when the long-range order vanishes that the correlation part of the Hubbard I self-energy becomes singular. Physically, it reflects the fact that these two approximations are valid in different limits, as discussed earlier. To resolve this problem, one has to go beyond the perturbation theory because one cannot get the Mott insulator by any local nonrenormalized perturbation expansion (NRPE) in U [55]. Indeed, within NRPE, we find the following self-energy for the homogeneous phase:

$$\Sigma_\sigma(\omega, \mathbf{k}; d = 0) = \frac{U}{2} + \frac{U/4}{\omega - \Delta_0(\omega)},$$

where the hybridization function $\Delta_0(\omega) = \omega - G_0^{-1}(\omega)$ and $G_0(\omega)$ is a noninteracting Green function at a single lattice site and is given by the Hilbert transform of a noninteracting density of states $G_0(\omega) = \int \rho_0(\omega)/(\omega - \epsilon)$. From the particle-hole symmetry, $G_0(0) = -i\pi\rho(0)$, where $\rho(0) = 0$ in our system. Hence $\Delta_0(\omega \to 0) = -i\infty$ and thereby at $\omega = 0$ the self-energy reduces to the Hartree self-energy.

The most advanced renormalized local approximation is the DMFT [33,34]. Our preliminary DMFT results [56] show that up to the critical interaction strength U_{c1}, the hybridization function at $\omega = 0$ is the same as within the Hartree approximation and the system is a topological insulator. Then, the metal-insulator transition occurs and the hybridization function has finite imaginary part. At the interaction strength $U_{c2} > U_{c1}$, the gap is opened again and the system becomes a topologically trivial Mott insulator with the hybridization function at $\omega = 0$ equal to zero as within the Hubbard I approximation. Hence the Hartree solution can be interpreted as an upper bound and the Hubbard I solution as a lower bound on the value of $U_{c1(2)}$, respectively. This result is consistent with a work [32] in which the DMFT equations where solved in the homogeneous phase.

V. THERMODYNAMIC PHASE DIAGRAM

The stability of the CDW phase is determined by a minimization of the free energy with respect to the order parameter d at a fixed temperature T and given microscopic

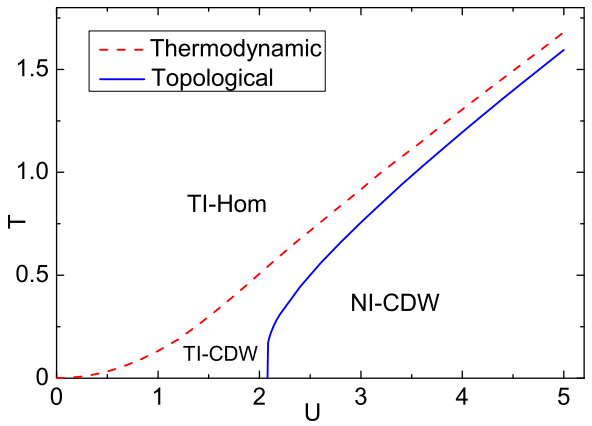

FIG. 4. (Color online) Phase diagram of KMFK model for $t_2 = 0.2$ within the Hartree approximation.

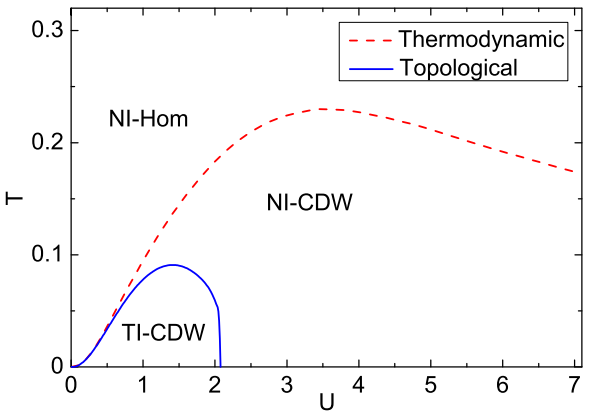

FIG. 5. (Color online) Phase diagram of the studied model for $t_2 = 0.2$ within Hubbard I approximation.

parameters U and t_2. The free energy of the KMFK model is [57]

$$F(d,T) = -\frac{2}{\beta}\int \rho(\omega;d)\ln(1+e^{-\beta\omega})d\omega + \frac{1}{\beta}[n_A \ln(n_A) + n_B \ln(n_B)], \tag{16}$$

where the first term describes a contribution from the itinerant electrons and is equivalent to the free energy of the noninteracting fermions but with a density of states $\rho(\omega;d)$ modified by the interaction. The second term describes an entropic contribution from the localized particles. The inverse of the temperature is denoted by $\beta = 1/T$. The temperature dependence of the topological phase transitions is obtained by inserting the optimal value $d(T)$ into the corresponding equations (12) and (15).

The thermodynamic and topological phases within the Hartree approximation are displayed in Fig. 4 for a selected value of $t_2 = 0.2$. There are three phases: a homogeneous topological insulator (TI-Hom), a topological insulator with the CDW long-range order (TI-CDW), and a normal insulator with the CDW long-range order (NI-CDW). The continuous thermodynamic transition between the TI-Hom and the TI-CDW is marked by the red dashed curve. The topological transition between the TI-CDW and the NI-CDW, displayed by the blue solid curve, is associated with closing a gap and a semimetallic behavior right at the transition line. Interestingly, the coexistence of the CDW long-range order and the topological phase occurs in a finite range of U values for a given temperature. This also contrasts to the Haldane model with nearest-neighbor interactions, where the charge-ordered phase is always topologically trivial [58]. Since at $T = 0$ the order parameter $d = 1$ for any U, we find from Eq. (12) that the TI-CDW - NI-CDW transition takes place at $U_c^{\mathrm{H}} = 6\sqrt{3}t_2$, which agrees with Fig. 4. For other t_2 hopping parameters, the phase diagrams are qualitatively similar to those presented in Fig. 4. However, when t_2 decreases, the coexistence TI-CDW regime shrinks and finally disappears at $t_2 = 0$ because it is t_2 that induces the topologically nontrivial phase.

The thermodynamic and topological phases within the Hubbard I approximation are displayed in Fig. 5 for the same t_2 as in the Hartree approximation above. There are again three but different phases: a homogeneous normal insulator (NI-Hom), TI-CDW, and NI-CDW. The homogeneous topological insulator, seen in Fig. 4, is replaced by the homogeneous normal insulator. The topological phase occurs together with the CDW long-range order and forms a bounded area on the phase diagram with a nonmonotonic behavior of the critical temperature. Again this is in contrast with the Haldane model with nearest-neighbor interactions, where the charge-ordered phase is topologically trivial [58]. We also note that at $T = 0$ the phase diagrams in Figs. 4 and 5 are identical. This is a general feature of the solutions of the KMFK model within local approximations to the self-energy.

The topological transition line in Fig. 5 has two characteristic behaviors: (i) for small U, the thermodynamic and topological lines are almost tangent to each other; and (ii) for U close to $U_c^{\mathrm{HI}} = 6\sqrt{3}t_2$ the topological line is almost vertical. The course of the topological line results from Eq. (15), which relates the critical interaction strength U_c^{HI} and the value of the order parameter $d(T)$ for which topological transition occurs. For temperatures close to the thermodynamic transition temperature T_c, the order parameter takes the form $d(T) \approx \alpha\sqrt{T - T_c(U)}$, where α is a constant. Substituting this function into Eq. (15) the topological transition temperature

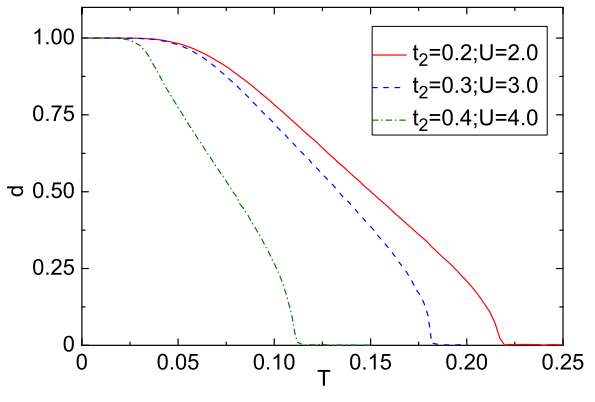

FIG. 6. (Color online) Order parameter as a function of the temperature for selected t_2 and U within the Hubbard I approximation.

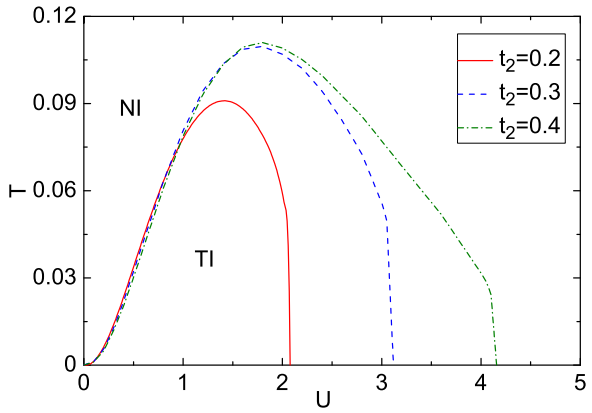

FIG. 7. (Color online) Topological phase diagrams of the KMFK model for selected t_2 within the Hubbard I approximation.

T_{top} is

$$T_{\text{top}} \approx T_c(U) + \frac{U^2}{108\alpha^2 t_2^2}. \tag{17}$$

Hence the topological critical temperature tends to the thermodynamic one, when U tends to zero and its main correction is of the order $O(U^2)$. In the second case, the topological line follows the course of the order parameter when its value approaches unity. At low temperatures, the order parameter is almost a constant, as is seen in Fig. 6, and this behavior gives rise to the vertical slope of the topological transition line in Fig. 5.

The topological phase diagrams for different t_2 are displayed in Fig. 7. When the hopping parameter increases, an area of the topological phase is extended. This originates from the fact that the hopping t_2 triggers the topological phases in the KMFK model (5). The height of the nearly vertical part of the topological line decreases because the constant part of the function $d(T)$ decreases with increasing t_2, as is seen in Fig. 6.

Comparing Figs. 4 and 5 we see that the critical temperature for the thermodynamic transition is reduced by the correlation effects taken into account in the Hubbard I approximation and becomes nonmonotonic. From Fig. 8, we see that the temperature of the thermodynamic transition decreases with increasing t_2 for each U.

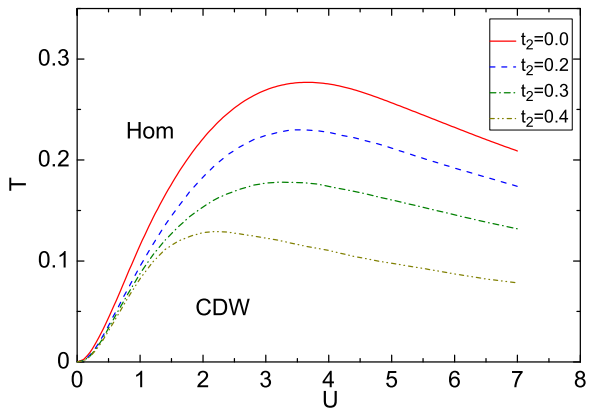

FIG. 8. (Color online) Thermodynamic phase diagrams of the KMFK model for selected t_2 within the Hubbard I approximation.

VI. CONCLUSION

In this paper, we studied correlation effects on the phase diagram of the topological insulator at finite temperatures. We started with the definition of topological phases of density matrices and using it we extended the concept of topological invariants to nonzero temperatures. We introduced a model that allows the existence of states with a long-range order, due to the interaction, and with nontrivial topology, due to a complex hopping amplitude. Using the concept of the topological Hamiltonian and the dynamical local approximation [33,34] to a many-body Hamiltonian, we found analytically the condition for the topological phase transition. Within the Hartree and the Hubbard I approximations, the complete phase diagrams with normal, topological, and long-range order phases were determined. The comparison of thermodynamic phase diagrams allows us to conclude that both the temperature and the interaction play a crucial role for the existence of nontrivial topological states and they should be included in realistic calculations. In particular, within the Hubbard I approximations, where the correlation effects are taken into account, the topological state appears only inside the CDW phase and is bounded to a finite area on the phase diagram. Moreover, the homogeneous phase is a topologically trivial Mott insulator. The Hubbard I approximation seems to be the simplest approximation that can describe a complete destruction of the topological phase only due to local correlations.

ACKNOWLEDGMENTS

We thank J. Tworzydlo for discussions. We acknowledge support from the Foundation for Polish Science (FNP) through the TEAM/2010-6/2 project, co-financed by the EU European Regional Development Fund.

APPENDIX A: STABILITY OF CDW PHASE

In the strong interaction limit, the KMFK model is mapped onto the antiferromagnetic Ising model, where $s_i = n_i - 1/2$ is a spin variable at a site i and the exchange coupling constants are $J_1 = t_1^2/4U$ for the nearest-neighbor and $J_2 = t_2^2/4U$ for the next-nearest-neighbor hopping, respectively [59,60]. On the honeycomb lattice, the ground state is a simple antiferromagnet for $J_2/J \leqslant 0.25$ and a superantiferromagnet otherwise [61]. Such spin configurations correspond to the checkerboard and stripes patterns of the localized particles, respectively. Hence, we obtain the threshold ratio $t_2/t_1 < 0.5$ of the CDW phase stability for arbitrary U. When it is not satisfied, the CDW phase can still exist but only in a finite range of U.

APPENDIX B: CHANGE OF THE TOPOLOGICAL INVARIANT

The topological invariant of the KMFK model (5) is equivalent to the Chern number for the spin-up copy of the

Haldane model [51]. The Chern number is defined by [6]

$$C = \frac{1}{2\pi}\int_{BZ} \Omega(\mathbf{k})\, d\mathbf{k}, \tag{B1}$$

where the surface integral is over the Brillouin zone (BZ), and $\Omega(\mathbf{k}) = \nabla_{\mathbf{k}} \times A(\mathbf{k})$ is a Berry curvature. The vector potential $A(\mathbf{k}) = -i\langle u(\mathbf{k})|\nabla_{\mathbf{k}}|u(\mathbf{k})\rangle$ is called a Berry connection and $|u(\mathbf{k})\rangle$ are eigenvectors of the lower block band of the Hamiltonian matrix (8). From Stokes theorem, we see that the Chern number is nonzero when one global gauge of the vector potential $A(\mathbf{k})$ does not exist. Therefore this observation yields a practical test of the existence of nontrivial topology.

In the KMFK model, the topological Hamiltonian matrix is given by a two-dimensional matrix that can be written in the form

$$H^{\text{top}}(\mathbf{k}) = H^x(\mathbf{k})\hat{\tau}^x + H^y(\mathbf{k})\hat{\tau}^y + H^z(\mathbf{k})\hat{\tau}^z, \tag{B2}$$

where the Pauli matrices are marked by τ^i with $i = x,y,z$ and the decomposition coefficients $H^i(\mathbf{k})$ are functions of the momentum. The spin index σ is omitted. For the two-dimensional Hamiltonian matrix, the eigenvector of the lower band, i.e., the eigenvalue for a given $\mathbf{k}$, is

$$u^I(\mathbf{k}) = \frac{1}{N^I}\begin{pmatrix} H^z(\mathbf{k}) - |H(\mathbf{k})| \\ H^x(\mathbf{k}) + iH_y(\mathbf{k}) \end{pmatrix}, \tag{B3}$$

where $|H(\mathbf{k})| = \sqrt{H^x(\mathbf{k})^2 + H^y(\mathbf{k})^2 + H^z(\mathbf{k})^2}$ and N^I is a normalization constant. This wave function is singular when $H^x(\mathbf{k}) = H^y(\mathbf{k}) = 0$ and $H^z(\mathbf{k}) > 0$. We can gauge out the singularity by performing a gauge transformation $u^I(\mathbf{k}) \to u^I(\mathbf{k})e^{i\phi(\mathbf{k})}$ obtaining the eigenvector

$$u^{II}(\mathbf{k}) = u^I(\mathbf{k})e^{i\phi(\mathbf{k})} = \frac{1}{N^{II}}\begin{pmatrix} -H^x(\mathbf{k}) + iH^y(\mathbf{k}) \\ H^z(\mathbf{k}) + |H(\mathbf{k})| \end{pmatrix}. \tag{B4}$$

It is now singular when $H^x(\mathbf{k}) = H^y(\mathbf{k}) = 0$ and $H^z(\mathbf{k}) < 0$. The vector $\vec{d}(\mathbf{k}) = (H^x(\mathbf{k}), H^y(\mathbf{k}), H^z(\mathbf{k}))/|H(\mathbf{k})|$ sets a map from the BZ into the two-dimensional unit sphere. If $\vec{d}(BZ)$ covers both poles of the sphere, there is no single gauge in the whole BZ to avoid the singularities.

For the KMFK model, $H^x = H^y = 0$ only at the Dirac points $\mathbf{K} = (4\pi/3\sqrt{3}a, 0)$ and $\mathbf{K}' = -\mathbf{K}$, where a is a lattice constant. At these points $H^z(\mathbf{K}) = \Sigma_R(d) - 3\sqrt{3}t_2$ and $H^z(\mathbf{K}') = \Sigma_R(d) + 3\sqrt{3}t_2$. Hence the vector $\vec{d}(\mathbf{k})$ contains only one pole for $\mathbf{k} \in$ BZ when the condition

$$|\Sigma_R(d)| > |3\sqrt{3}t_2| \tag{B5}$$

is fulfilled and therefore the system is in the topologically trivial phase.

[1] C. L. Kane and E. J. Mele, Phys. Rev. Lett. **95**, 226801 (2005).
[2] C. L. Kane and E. J. Mele, Phys. Rev. Lett. **95**, 146802 (2005).
[3] L. Fu, C. L. Kane, and E. J. Mele, Phys. Rev. Lett. **98**, 106803 (2007).
[4] B. A. Bernevig, T. L. Hughes, and S.-C. Zhang, Science **314**, 1757 (2006).
[5] L. Fu and C. L. Kane, Phys. Rev. B **76**, 045302 (2007).
[6] M. Z. Hasan and C. L. Kane, Rev. Mod. Phys. **82**, 3045 (2010).
[7] X. L. Qi and S. C. Zhang, Rev. Mod. Phys. **83**, 1057 (2011).
[8] J. C. Budich and B. Trauzettel, Phys. Status Solidi RRL **7**, 109 (2013).
[9] M. Konig, S. Wiedmann, C. Brune, A. Roth, H. Buhmann, L. W. Molenkamp, X. L. Qi, and S. C. Zhang, Science **318**, 766 (2007).
[10] P. Dziawa, B. J. Kowalski, K. Dybko, R. Buczko, A. Szczerbakow, M. Szot, E. Łusakowska, T. Balasubramanian, B. M. Wojek, M. H. Berntsen, O. Tjernberg, and T. Story, Nat. Mater. **11**, 1023 (2012).
[11] H. Peng, K. Lai, D. Kong, S. Meister, Y. Chen, X.-L. Qi, S.-C. Zhang, Z.-X. Shen, and Y. Cui, Nat. Mater. **9**, 225 (2010).
[12] J. G. Checkelsky, Y. S. Hor, M. H. Liu, D.-X. Qu, R. J. Cava, and N. P. Ong, Phys. Rev. Lett. **103**, 246601 (2009).
[13] D. Hsieh *et al.*, Nature (London) **452**, 970 (2008).
[14] D. Hsieh *et al.*, Phys. Rev. Lett. **103**, 146401 (2009).
[15] Y. Xia *et al.*, Nat. Phys. **5**, 398 (2009).
[16] M. Hohenadler and F. F. Assaad, J. Phys.: Condens. Matter **25**, 143201 (2013).
[17] S. Raghu, Xiao-Liang Qi, C. Honerkamp, and S.-C. Zhang, Phys. Rev. Lett. **100**, 156401 (2008).
[18] L. Wang *et al.*, arXiv:1012.5163.
[19] J. C. Budich, B. Trauzettel, and G. Sangiovanni, Phys. Rev. B **87**, 235104 (2013).
[20] J. C. Budich, R. Thomale, G. Li, M. Laubach, and S.-C. Zhang, Phys. Rev. B **86**, 201407(R) (2012).
[21] S. Rachel and K. Le Hur, Phys. Rev. B **82**, 075106 (2010).
[22] A. Shitade, H. Katsura, J. Kunes, X.-L. Qi, S. C. Zhang, and N. Nagaosa, Phys. Rev. Lett. **102**, 256403 (2009).
[23] G. Jotzu *et al.*, Nature (London) **515**, 237 (2014).
[24] I. Bloch, J. Dalibard, and W. Zwerger, Rev. Mod. Phys. **80**, 885 (2008).
[25] V. Galitski and I. B. Spielman, Nature (London) **494**, 49 (2013).
[26] Y.-X. Zhu *et al.*, J. Phys.: Condens. Matter **26**, 175601 (2014).
[27] Y.-H. Chen, H.-H. Hung, G. Su, G. A. Fiete, and C. S. Ting, Phys. Rev. B **91**, 045122 (2015).
[28] T. Yoshida, S. Fujimoto, and N. Kawakami, Phys. Rev. B **85**, 125113 (2012).
[29] W. Wu, S. Rachel, W. M. Liu, and K. Le Hur, Phys. Rev. B **85**, 205102 (2012).
[30] J. C. Budich and S. Diehl, Phys. Rev. B **91**, 165140 (2015).
[31] L. M. Falicov and J. C. Kimball, Phys. Rev. Lett. **22**, 997 (1969).
[32] H.-S. Nguyen and M.-T. Tran, Phys. Rev. B **88**, 165132 (2013).
[33] W. Metzner and D. Vollhardt, Phys. Rev. Lett. **62**, 324 (1989).
[34] A. Georges, G. Kotliar, W. Krauth, and M. J. Rozenberg, Rev. Mod. Phys. **68**, 13 (1996).
[35] A. P. Schnyder, S. Ryu, A. Furusaki, and A. W. W. Ludwig, Phys. Rev. B **78**, 195125 (2008).
[36] J. C. Budich, P. Zoller, and S. Diehl, Phys. Rev. A **91**, 042117 (2015).
[37] S. Diehl, E. Rico, M. A. Baranov, and P. Zoller, Nat. Phys. **7**, 971 (2011).

[38] Z. Wang, X.-L. Qi, and S.-C. Zhang, Phys. Rev. Lett. **105**, 256803 (2010).
[39] Z. Wang and S.-C. Zhang, Phys. Rev. X **2**, 031008 (2012).
[40] Z. Wang and B. Yan, J. Phys.: Condens. Matter **25**, 155601 (2013).
[41] Z. Huang and D. P. Arovas, Phys. Rev. Lett. **113**, 076407 (2014).
[42] O. Viyuela, A. Rivas, and M. A. Martin-Delgado, Phys. Rev. Lett. **113**, 076408 (2014).
[43] Y. Ran, A. Vishwanath, and D.-H. Lee, Phys. Rev. Lett. **101**, 086801 (2008).
[44] X.-L. Qi and S.-C. Zhang, Phys. Rev. Lett. **101**, 086802 (2008).
[45] F. F. Assaad, M. Bercx, and M. Hohenadler, Phys. Rev. X **3**, 011015 (2013).
[46] B. M. Wojek, P. Dziawa, B. J. Kowalski, A. Szczerbakow, A. M. Black-Schaffer, M. H. Berntsen, T. Balasubramanian, T. Story, and O. Tjernberg, Phys. Rev. B **90**, 161202 (2014).
[47] J. E. Hirsch, Phys. Rev. Lett. **83**, 1834 (1999).
[48] F. D. M. Haldane, Phys. Rev. Lett. **61**, 2015 (1988).
[49] T. Kennedy and E. H. Lieb, Physica A **138**, 320 (1986).
[50] J. Wojtkiewicz, J. Stat. Phys. **123**, 585 (2006).
[51] For the Haldane model, the Chern number $C = \pm 1$ depends on the sign of the Peierls phase [48]. In the case of the system from Eq. (5), the total Chern number is a sum of Chern numbers for both copies of the Haldane model $C = C_\uparrow + C_\downarrow = 0$. However, we can define a new topological invariant connected with the conservation of the perpendicular spin S_z. It is called the spin Chern number [1] and is given by the formula $C_s = \frac{C_\uparrow - C_\downarrow}{2}$. Hence, for our model, it is equal to the Chern number of a single copy of the Haldane model $C_s = C_\uparrow$. The topological invariant υ of the time reversal symmetry is linked to the spin Chern number by the equation $\upsilon = C_s \mod 2$ [6].
[52] B. A. Bernevig and T. L. Hughes, *Topological Insulators and Topological Superconductors* (Princeton University Press, Princeton, 2013), pp. 30–32.
[53] F. Gebhard, *The Mott Metal-insulator Transition: Models and Methods* (Springer, Berlin, Heidelberg, 1997), pp. 270–274.
[54] L. Wang, Xi Dai, and X. C. Xie, Phys. Rev. B **84**, 205116 (2011).
[55] T. D. Stanescu, P. W. Phillips, and T.-P. Choy, Phys. Rev. B **75**, 104503 (2007).
[56] D. Zdulski and K. Byczuk (unpublished).
[57] A. M. Shvaika and J. K. Freericks, Phys. Rev. B **67**, 153103 (2003).
[58] C. N. Varney, K. Sun, M. Rigol, and V. Galitski, Phys. Rev. B **84**, 241105(R) (2011).
[59] Umesh K. Yadav, T. Maitra, and Ishwar Singh, Solid State Commun. **164**, 32 (2013).
[60] Ch. Gruber, N. Macris, A. Messager, and D. Ueltschi, J. Stat. Phys. **86**, 57 (1997).
[61] A. O'Hare, F. V. Kusmartsev, and K. I. Kugel, Int. J. Mod. Phys. B **23**, 3951 (2009).